EurJIC European Journal of Inorganic Chemistry

MICROREVIEW

DOI: 10.1002/ejic.201101056

MOFs for Use in Adsorption Heat Pump Processes

Stefan K. Henninger,*[a] Felix Jeremias,[a] Harry Kummer,[a] and Christoph Janiak[b]

Keywords: Metal–organic frameworks / Adsorption / Thermochemistry / Heat pumps / Solar cooling

Thermally driven heat pumps can significantly help to minimize primary energy consumption and greenhouse gas emissions generated by industrial or domestic heating and cooling processes. This is achieved by using solar or waste heat as the operating energy rather than electricity or fossil fuels. One of the most promising technologies in this context is based on the evaporation and consecutive adsorption of coolant liquids, preferably water, under specific conditions. The efficiency of this process is first and foremost governed by the microporosity, hydrophilicity, and hydrothermal stability of the sorption material employed. Traditionally, inorganic porous substances like silica gel, aluminophosphates, or zeolites have been investigated for this purpose. However, metal–organic frameworks (MOFs) are emerging as the newest and by far the most capable class of microporous materials in terms of internal surface area and micropore volume as well as structural and chemical variability. With further exploration of hydrothermally stable MOFs, a large step forward in the field of sorption heat pumps is anticipated. In this work, an overview of the current investigations, developments, and possibilities of MOFs for use in heat pumps is given.

Introduction

The principle of sorptive cooling has a long-lasting history, dating back to Faraday in 1848, who used ammonia and silver chloride as the working pair.[1] With increasing concerns over ozone depletion and the global warming potential of CFCs and HFCs, augmented energy demand and the resulting CO_2 emissions, the interest in energy-efficient systems and especially new cooling and heating technologies that make use of environmentally friendly refrigerants has grown rapidly. In addition, there is an increasing energy demand for summer air-conditioning due to increased thermal loads, higher living standards as well as architectural trends. Solar assisted air conditioning systems have been proposed as an alternative to conventional, vapor-compression-driven systems, as operation of the former requires almost no electrical power nor questionable refrigerants.[2] With regard to the large amount of available but unused low-temperature heat, either by solar thermal collectors or especially waste heat from industrial processes, thermally driven adsorption chillers (TDCs) or adsorption heat pumps (AHPs) provide a promising approach towards a more efficient use of low-temperature heat and an effective climate protection. The central idea for solar cooling systems is the very good direct correlation between solar irradiation, and therefore the supply of solar energy, and the cooling demand of buildings.

[a] Department of Thermally Active Materials and Solar Cooling, Fraunhofer Institute for Solar Energy Systems (ISE), Heidenhofstr. 2, 79110 Freiburg, Germany
Fax: +49-761-4588-9000
E-mail: stefan.henninger@ise.fraunhofer.de
[b] Institut für Anorganische Chemie und Strukturchemie, Universität Düsseldorf, 40204 Düsseldorf, Germany

Working Principle

The working principle of solid sorption heat transformation systems in view of basic thermodynamics can be described as a combination of a heat engine and a heat pump, where the work produced by the heat engine is used to run the heat pump cycle. Therefore, the thermodynamic limit can be described by a Carnot cycle, consisting of three temperatures. The underlying basic principle is illustrated in Figure 1. Basically, the sorption system exchanges the re-

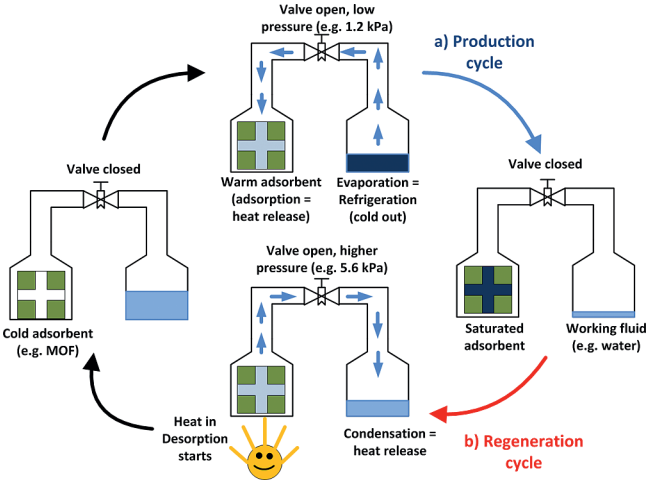

Figure 1. Illustration of the basic principle for adsorption chillers or heat pumps.

frigerant vapor between the evaporator/condenser and the adsorbent. This can be further divided into a production or heat pump cycle and a regeneration or heat engine cycle. As the most important property of the working fluid is its specific evaporation enthalpy, water is used preferably, but it is also possible to use other fluids for special purposes. Within the production cycle, the working fluid is evaporated; thereby cold is produced in the cooling case or heat is extracted from a low-temperature heat source in the heat pump application. Then the water vapor is adsorbed by the porous material, which causes heat to be released at a medium temperature level. This is useful heat in the heat pump application or is simply released to the environment in the cooling case.

In the regeneration phase, the porous material is heated by, for example, a gas burner, solar, thermal, or waste heat, and the adsorbed water is released, condensing again at a medium temperature level. The heat of condensation is useful heat in the heat pump case or released to the environment in the cooling case. It is not the aim of this paper to give a comprehensive review of the sorption thermodynamics and technology. The interested reader is referred to the extensive literature in this field.[1–8]

MOFs as Adsorption Materials

Despite the impressive progress that has been achieved on materials for use in adsorptive heat transformation, the discovery of new microporous materials for use in adsorption heat pump processes is still a fundamental research topic with exciting improvements and numerous publications.[9–11] In addition to inorganic materials like zeolites and aluminophosphates, a new class of microporous materials well known as porous coordination polymers (PCPs) or metal–organic frameworks (MOFs) has emerged.[12–22]

These materials possess unique features such as huge surface area, large pore volume, and an unprecedented geometric, chemical, and physicochemical variability, which are due to their tunable composition. So far, MOFs have been mainly considered for storage of light gases like hydrogen or methane,[23–26] for gas separation purposes,[27–32] and for catalytic,[33–37] optical,[38–40] magnetic,[41–43] and other applications.[17,24,44–46] So far, water adsorption has been treated as an unrequested side effect of hydrogen or methane adsorption. Even more problematic is the need to exclude water rigorously, as many MOFs, in particular the {Zn_4O}-IRMOF-n series, are unstable in the presence of

Stefan Henninger studied physics at the University of Freiburg, where he graduated in collaboration with the Fraunhofer ISE in 2002. He did his PhD work at the Freiburg Material Research Center (FMF) from 2003 to 2007, using computer simulation to identify different adsorbents for heat storage and transformation applications by Monte Carlo methods of water adsorption. In January 2008, he returned to the Fraunhofer ISE, and he has been Team Manager of "Sorption Technology – Material Development and Characterization" since 2009. His current research projects include the development of new sorption materials, characterization and thermodynamic description of the adsorption process, as well as coatings of these materials on different supports.

Felix Jeremias studied chemistry at the University of Konstanz and graduated in 2010 with work on reactions on mesoporous organosilica. Currently, he is doing his PhD Thesis with Prof. Janiak (University of Düsseldorf) in close collaboration with the sorption materials team at Fraunhofer ISE, investigating the suitability, synthesis, and properties of coordination polymers for heat transformation applications.

Harry Kummer studied chemistry at the Albert-Ludwigs University of Freiburg with focus on macromolecular chemistry. He did his diploma thesis in collaboration with the Fraunhofer ISE and works on coatings for heat exchangers in adsorption systems. Since 2009 he is a member of the Team of Stefan Henninger "Sorption Technology – Material and Development" at the Fraunhofer ISE in Freiburg.

Christoph Janiak studied chemistry at the Technical University Berlin (TUB) and the University of Oklahoma with a Diploma and a M.Sc. graduation in 1984. He obtained his PhD at the TUB under Prof. Herbert Schumann in 1987, followed by postdoctoral stays at Cornell University with Prof. Roald Hoffmann and at BASF AG, Ludwigshafen in the polyolefin division. From 1991 to 1995 he carried out his Habilitation at the TUB. In 1996 he took a temporary professorship at the University of Freiburg, where he became C3 professor for Inorganic and Analytical chemistry (1998–2010). In November 2010 he moved to Düsseldorf to a Chair for Bioinorganic Chemistry and Catalysis. His research interests are porous coordination polymers or metal–organic frameworks, metal nanoparticles, and catalysis.

water impurities over several gas sorption cycles.[47] Consequently, water adsorption measurements are now performed in order to investigate structural properties like pore size and stability of pore volume in the presence of water vapor.[48] It is beyond the scope of this paper to give a comprehensive overview on the available structures and possible applications that can be found in extensive reviews.[15,17,46,49–52]

With regard to the application in adsorption heat transformation processes, the main focus lies on water adsorption properties and storage capacities, which are strongly connected to the specific pore volume. With ongoing development, the specific pore volumes have increased from 1 $cm^3 g^{-1}$ (MOF-5) up to more than 2 $cm^3 g^{-1}$ for MIL-101.[53] In combination with increasing pore volumes, extremely high surface areas up to 5000 $m^2 g^{-1}$ have been reported for several MOFs. This has also started a discussion on the applied measurement methods, for example, the determination of the surface area by the BET method.[54]

Another unique feature can be observed when dealing with the adsorption properties of MOFs. Some frameworks show geometric flexibility, that is, a reversible change in the structure and sometimes even in the physical properties in response to guest adsorption. This "breathing" effect can be observed for several structures and for all dimensionalities, and it can lead to a stepwise adsorption of water, or, even more interestingly, to the phenomenon of a switching system. As reported by Tanaka et al., this so-called gate effect occurs during the adsorption process itself, when the MOF structure changes from a "closed" to an "open" structure at a specific gate pressure.[55] Recently, this guest-induced structural transition has been explained with a general thermodynamic approach, although not for water but for a large variety of gases, by Coudert and co-workers.[56] In case of the water-induced transition, Coombes et al. studied the breathing effect of MIL-53 with DFT and force-field-based simulations.[57] The resulting adsorption isotherm has an S-like shape, which is advantageous for the applications in focus of this work. However, the repeated expansion and shrinkage of the framework leads to several problems such as discontinuities at high relative pressures or large hysteresis. Furthermore, the framework itself can be destroyed as a result of the significant stress on the coordinative bonds during the structural transformation.

Compared to traditional adsorbents used in heat pump applications, like zeolites or aluminophosphates, MOFs exhibit a much richer variety in terms of composition, pore structure, and topology. The underlying cluster/linker concept allows the tuning of pore structures and chemical functionalities over a wide range. Another advantage is the mechanism of synthesis: The solvent itself acts as the main template in contrast to the templated synthesis of, for example, SAPO-34, in which a high-temperature activation process is needed to remove, for example, the tetraethyl ammonium hydroxide template in order to generate the porosity. For applications in periodically working heat pumps or adsorption chillers, the comparatively weak thermal and especially hydrothermal stability of MOFs can be a disadvantage and is the most critical issue.[58] The most crucial point for hydrothermal stability is the nature of the metal–ligand coordinative bond: Hydrothermal decomposition is usually initiated by substitution of the linker with water molecules, and several metal–linker combinations, for example, zinc–carboxylate, have proven generally unstable towards water (e.g. IRMOFs, MOF-5, DUT-4).[47,59] Mainly because of the organic matter incorporated in the construction of MOFs, the long-time thermal metal–ligand framework stability lies typically between 150–250 °C and seldom surpasses 300 °C. This is much less than values known for zeolites.

Thermodynamic Boundaries

With regard to heat transformation cycles, some general requirements for the adsorption equilibria, and hence for the applied sorption material, can be formulated. The first figure of merit is the achievable water loading lift, more precisely the working fluid exchange between the production cycle (adsorption) and the regeneration cycle (desorption). This exchange can be described as the difference between the richest and the weakest isostere of the cycle in an Arrhenius diagram as illustrated in Figure 2.[60] In the thermodynamic context, the term *isosteric* denotes a process that occurs at a constant water loading, that is, without adsorption or desorption. In case of the cooling application, the cooling enthalpy produced in one cycle can simply be calculated as evaporation enthalpy times the working fluid exchange. The cycle is defined by the highest desorption temperature (driving temperature, point D), the minimum adsorption temperature (point B), and the condenser and evaporator pressure. The selection of the two pressure levels is geared to the possible applications. The pressure level of 1.2 kPa corresponds to an evaporation temperature of 10 °C, which marks a useful temperature level for cooling applications. The second pressure level of 5.6 kPa corre-

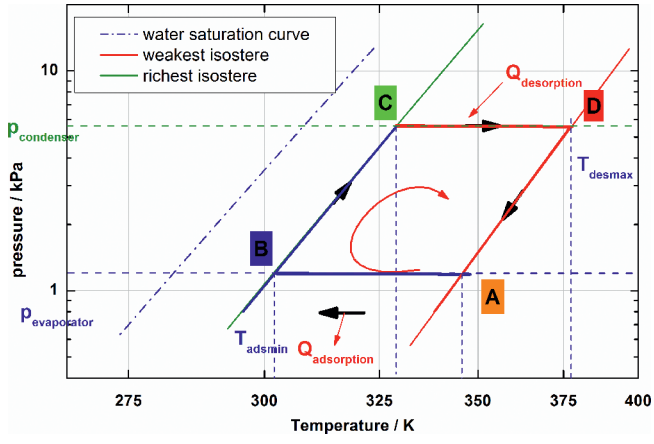

Figure 2. The van 't Hoff diagram of the ideal cycle. Reprinted with permission from ref.[60] Copyright 2011 Wiley-VCH Verlag GmbH & Co. KGaA.

sponds to 35 °C, which either marks the temperature at which heat can be released (cooling application) or can be used for low-temperature heating (heat pump application).

In an ideal cycle, adsorption and desorption are supposed to be an isobaric process. Hence the evaluation of materials for this type of application is realized by measurement of two isobars corresponding to the condenser and evaporator pressure. The ideal cycle in Figure 2 is displayed with the corresponding points as two isosteres with load 0.1 (weakest) and 0.4 (richest) (cf. Figure 3), leading to a reachable loading lift within the cycle of 0.3 g g^{-1}, which makes a good benchmark. The maximum desorption temperature (104 °C, point D) and the minimum adsorption temperature (28 °C, point B) define the relative pressure window between 0.05 and 0.32 (cf. Figure 3), in which a maximum load has to be reached.

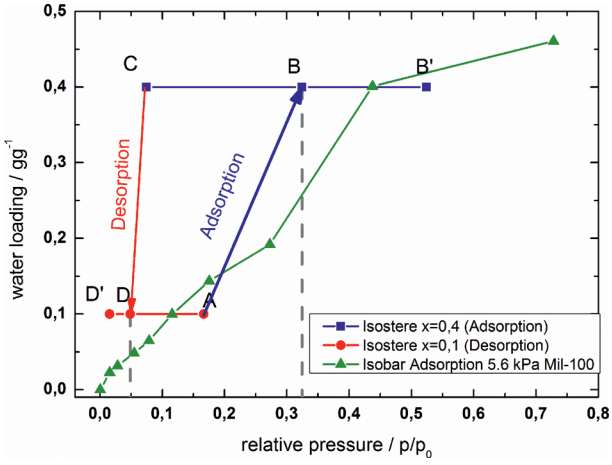

Figure 3. Illustration of a chiller cycle with the data for MIL-100(Fe).

However, as isothermal measurements are sometimes handier, the boundary conditions can be transformed to relative pressures as illustrated in Figure 3. In addition, an isobaric adsorption measurement at 5.6 kPa on a MIL-100(Fe) sample is displayed. As can be seen, the MIL-100(Fe) fits the requirements for the desorption step quite well, with a lower loading compared to that of the model material. However, if the minimal adsorption temperature can be lowered to 20 °C (point B′), the water exchange or loading lift that can be reached within this cycle is approximately 0.4 g g^{-1}.

As a first result out of these considerations, the strong dependence of the working window on the cycle conditions and the potential performance of MOFs for this application has been shown, which encourages further evaluation.

Potential of MOFs for Water Adsorption Processes

Isobars or isotherms for the adsorption of water on MOFs are still scarce. The first investigations of the suitability of MOFs for the use as adsorption material for heat transformation applications have shown their high potential, but also some critical issues.[61] An illustration of the high potential of MOFs for this application is given in Figure 4. The water uptake of MOFs easily outperforms that of any conventional material such as silica gel, zeolites, or SAPO/AlPO.

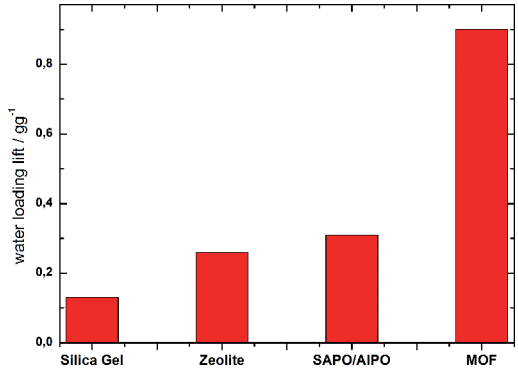

Figure 4. Illustration of the possible water loading lift for different material classes within a typical heat transformation cycle.

On the basis of the available literature, several promising candidates were identified and synthesized for the direct investigation of water sorption. In addition, three commercially available samples produced by BASF were evaluated.

Evaluation of HKUST-1

One of the first 3-dimensional porous MOFs, namely 3D-{[$Cu_3(btc)_2(H_2O)_3$]•~10H_2O} (btc = benzene-1,3,5-tricarboxylate), also called HKUST-1 or just Cu-BTC, was evaluated for use in heat transformation applications.[11,61,62] HKUST-1 consists of a basic building unit containing two central Cu^{2+} ions that are coordinated by four trimesate molecules through their carboxylate groups to form the paddlewheel-like structure of copper acetate $Cu_2(CH_3COO)_4(H_2O)_2$ (see Figure 5). With this building unit, a cubic structure can be realized. This MOF has been widely investigated for different applications as well as having been used as a model MOF for detailed simulations to understand guest–framework interactions.[63] Recently, molecular simulations of water in Cu-BTC were reported. They reveal different adsorption sites and especially the strong influence of the unsaturated Cu sites.[64–66]

The adsorption characteristics of various HKUST-1 samples synthesized at ISE are shown in comparison with data from Küsgens et al.[48] in Figure 6. Sample 1 shows the best agreement with the calculated data by Küsgens et al. as well as the highest loading spread within the ISE samples. This sample was synthesized with high-purity ethanol, whereas samples 2 and 3 were synthesized with technical ethanol with regard to eventual upscaling. The maximum water uptake of the HKUST-1 sample by Küsgens is 0.55 g g^{-1} for a relative pressure of p/p_0 = 0.9.

The adsorption characteristics are advantageous for the application, with a large loading in the relative pressure range 0.1 ≤ p/p_0 ≤ 0.4. In addition to these samples, a

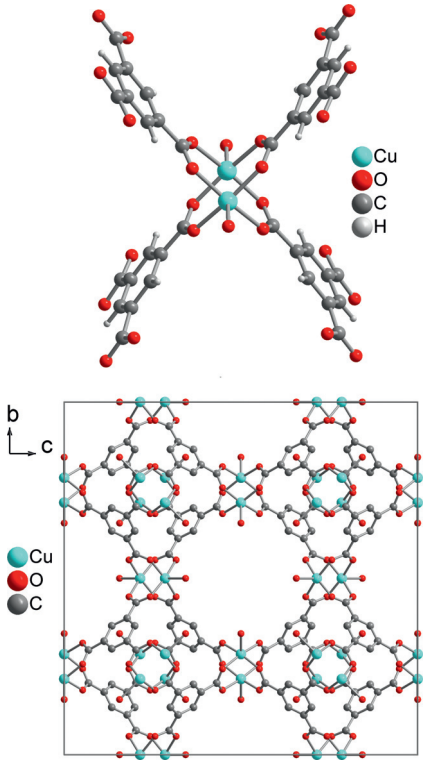

Figure 5. $\{Cu_2(btc)_4\}$ building unit and packing diagram with the cubic unit cell of 3D-$\{[Cu_3(btc)_2(H_2O)_3]\cdot\sim 10H_2O\}$ (water of crystallization not shown).

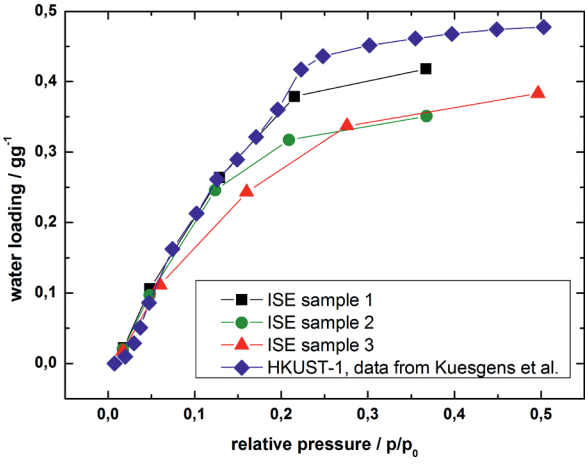

Figure 6. Water adsorption characteristics of different HKUST-1 (Cu-BTC) samples. ISE sample 1 was synthesized with high purity ethanol, whereas the samples 2 and 3 were synthesized with technical ethanol.

commercially available HKUST-1, namely Basolite™ C300 supplied by Sigma–Aldrich, was evaluated. The results are given further below.

The results of isobaric and isothermal measurements are given in Figure 7. In addition to thermogravimetric measurements, volumetric measurements were also performed, with very good agreement between the two measurement methods. In case of thermogravimetry, isobaric measurements at 1.2 kPa and 5.6 kPa were performed, which corresponds to the cycle conditions given above.

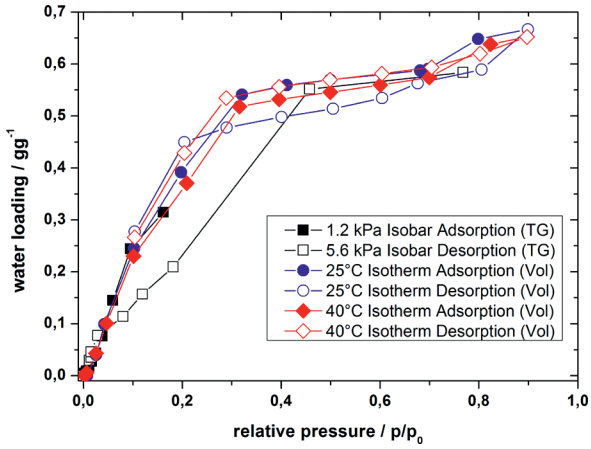

Figure 7. Water adsorption characteristics of Basolite™ C300. Measurements were performed with volumetric (Vol) and thermogravimetric (TG) methods.

The isothermal measurements were performed volumetrically at 25 °C and 40 °C in order to calculate the heat of adsorption. The commercially available HKUST-1 shows an even higher water uptake compared to that reported by Küsgens,[48] which may be attributed to more suitably optimized conditions of synthesis and purification, resulting in cleaner pores and a better phase purity. The adsorption characteristics are similar, with a large loading step in the relative pressure range $0.1 \leq p/p_0 \leq 0.4$, followed by a plateau.

The possible loading lift within a typical heat transformation cycle is in the range from 0.3 $g\,g^{-1}$ up to 0.5 $g\,g^{-1}$, which is considerably larger than those of currently used materials like silica gel or zeolites. Even SAPO-34, which has been the most promising material for AHPs so far, is outperformed. While these results are very promising for application in adsorption heat transformation systems, the hydrothermal stability is not yet sufficient. As reported before,[11,47,48,58,67] the framework shows irreversible structural changes during water adsorption/desorption over a few cycles. However, new synthesis methods may yield a material with improved thermal stability, as reported earlier.[68]

Evaluation of ISE-1

Another early example of a MOF evaluated as a potential adsorbent for low-temperature heating and cooling applications was 3D-$\{[Ni_3(\mu_3\text{-btc})_2(\mu_4\text{-btre})_2(\mu\text{-}H_2O)_2]\cdot\sim 22H_2O\}$ (ISE-1), featuring benzene-1,3,5-tricarboxylate (btc) and 1,2-bis(1,2,4-triazol-4-yl)ethane (btre) as organic ligands (Figure 8). ISE-1 is filled with approximately 22 water molecules per formula unit to yield a potential solvent volume of 1621 $Å^3$ (52% of the unit cell volume).[69]

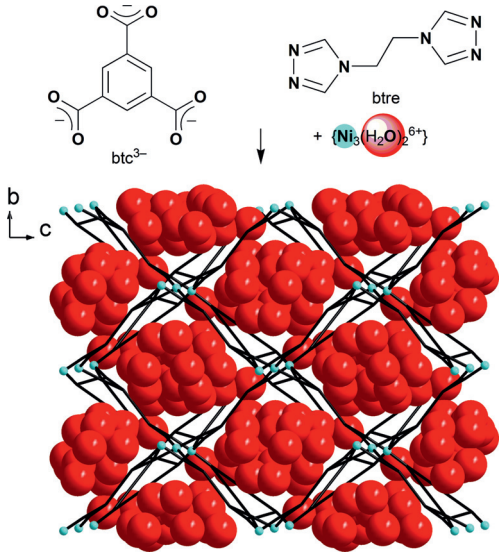

Figure 8. Schematic drawing of the ISE-1 MOF and the organic ligands used. Ligands btc and btre are depicted schematically as black lines only, nickel atoms as light blue spheres, and oxygen atoms of the guest/solvent water molecules as red space-filling spheres.

Although the reported water loading lift is significantly smaller, with a maximum of 0.21 g g^{-1}, this sample is stable over several water adsorption and desorption cycles, which shows the possibility, in principle, of the use of MOFs for water adsorption systems.

Evaluation of MIL-101 and MIL-100

MIL-101, developed at and named after the (Material) Institut Lavoisier, has turned out to be a very promising candidate.[16] MIL-101 is by now one of the best known and most cited MOFs. The crystalline mesoporous material 3D-{[$Cr_3(O)(bdc)_3(X)(H_2O)_2$]·~25$H_2O$}, bdc = benzene-1,4-dicarboxylate (terephthalate), X = F or OH depending on synthesis conditions, is a chromium(III) terephthalate with inner free-cage diameters of up to 34 Å (Figure 9). The framework is similar to the MZN zeolite topology.

Water adsorption isobars and isotherms were measured by using thermogravimetric and volumetric methods. These results, as well as a direct comparison with measurements performed independently by Quantachrome, have recently been published.[60] With an impressive water loading spread of 0.939 g g^{-1} under typical conditions (desorption at 90 °C, adsorption at 40 °C, vapor pressure 5.6 kPa), this material shows the largest water-loading spread reported so far. Similar water uptake isotherms at lower temperatures with a maximum water uptake of 1.37 g g^{-1} (although not under cycle conditions) have been reported by Küsgens et al.[48] Several isotherms for MIL-101(Cr), including data extracted from refs.[48,60] and a newly synthesized sample, are compared in Figure 10, proving the high water loading capacity of MIL-101(Cr) with a maximum uptake of up to 1.43 g g^{-1}.

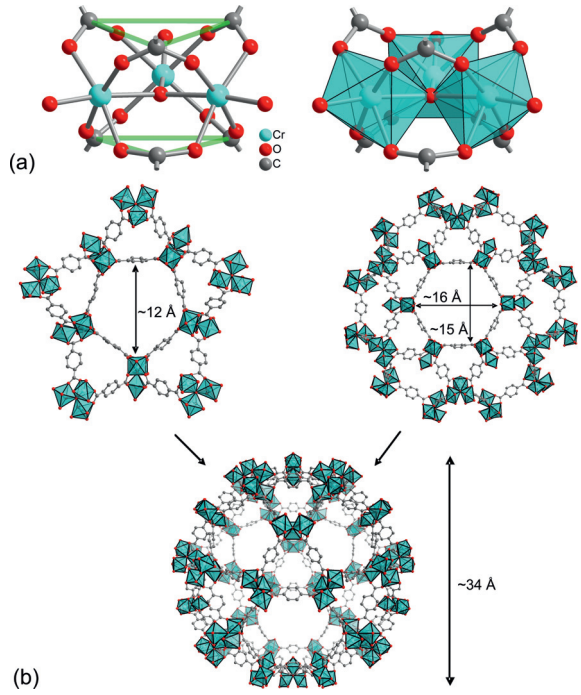

Figure 9. (a) Ball-and stick and polyhedral presentation of the trigonal-prismatic [$Cr_3(O)(F,OH)(H_2O)_2$] secondary building unit in 3D-[$Cr_3(O)(bdc)_3(F,OH)(H_2O)_2$]·~25$H_2O$, MIL-101. (b) Connectivity of the trigonal, pentagonal, and hexagonal ring systems to yield up to 34 Å large pores in the 3D framework structure. The individual pictures in this figure are not drawn to scale. (water of crystallization not shown).

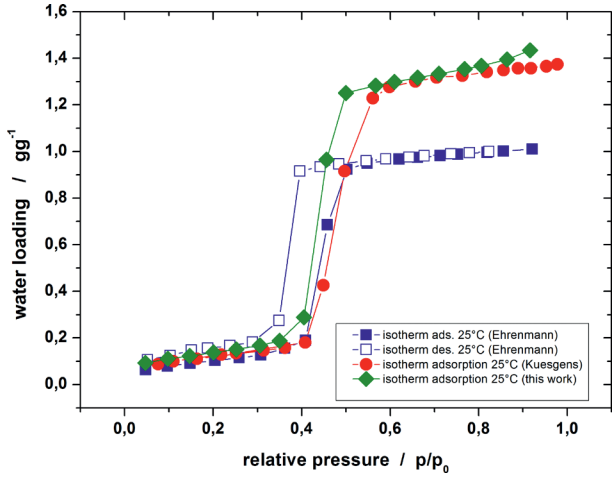

Figure 10. Water adsorption and desorption isotherms of different MIL-101(Cr) samples. This compound shows the highest water uptake of up to 1.43 g g^{-1}. (Isotherms from Ehrenmann,[60] calculated data from Küsgens,[48] and in addition a newly synthesized sample showing the highest water uptake.)

The isotherm of the compound shows a sigmoidal shape with a single adsorption step. This is advantageous for the application, as a large loading lift can be achieved within a narrow range of relative pressure. The existence of just one single step is surprising, as there are two pore types with window openings of 1.2 and 1.6 nm, which should be filled

consecutively. As suggested by Küsgens et al., this behavior originates from the similar hydrophilicity of the pores.

Unfortunately, the usable loading lift in the application is slightly reduced because of the small hysteresis between adsorption and desorption. The first experiments on hydrothermal stability have been performed with very promising results, showing only a slight degradation of approximately 3% compared to the initial load after 40 cycles.

A general overview with an excellent steam stability map of several porous coordination polymers can be found in the report by Low et al.[47] The MIL-101(Cr) compound has been classified into the high steam stability region with an activation energy for ligand displacement of 43.4 kcal mol^{-1} and a structural stability of up to 300 °C. These results back up the first cycling tests.

As a second candidate, the compound MIL-100(Cr)[70,71] was evaluated. This compound, with formula 3D-{[$Cr_3(O)(btc)_2(X)$]•~28H_2O} (X = F, Cl, 0.5SO_4), has also attracted attention as a promising adsorbent for water adsorption. Isostructural compounds featuring Fe^{3+} or Al^{3+} instead of Cr^{3+} can also be obtained,[72] and data for MIL-100(Fe)[48] will be discussed, too. As expected from the close relation between the two MOFs, both the maximum uptake (m = 0.8 g g^{-1}) and the shapes of the water sorption isotherms of MIL-100(Cr) and MIL-100(Fe) are almost identical (Figure 11). The adsorption isotherm can be divided into several steps, which have been explained with different mechanisms.[48] For $p/p_0 < 0.25$, mono- and multilayer adsorption of water molecules occurs mainly around the hydrophilic metal ion clusters. Capillary condensation can be observed in two steps, starting at p/p_0 = 0.25. Water molecules are adsorbed in the smaller cages with 2.5 nm diameter. The steep adsorption step between the relative pressure range from 0.3 to 0.4 can be attributed to the filling of the larger pores with diameter 2.9 nm. The following plateau is reached, as for MIL-101, at a relative pressure of 0.5 with a slight additional increase for higher relative pressures. The inner cage diameters and the window openings of the pores of MIL-100(Fe) are smaller than those of MIL-101.

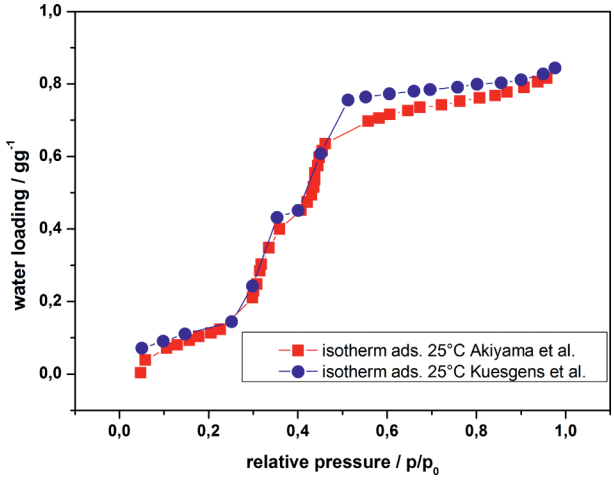

Figure 11. Water adsorption and desorption isotherms/isobars of MIL-100(Cr) by Akiyama et al.[71] and MIL-100(Fe) by Küsgens et al.[48]

Unlike MIL-101, MIL-100 shows only a small hysteresis between the adsorption and the desorption path, which may be attributed to both the smaller pores and the more strongly polar nature of the linker. Furthermore, Akiyama et al.[71] performed a stability test on this compound with two thousand cycles. No effect on the adsorption capacity was observed. Hence, this compound is of great interest for use in adsorption processes, although the feasible water loading spread is approximately 0.4 g g^{-1} for typical application conditions, which is smaller than that of the previously discussed MIL-101.

Evaluation of Basolite™ A100 [MIL-53(Al)] and Basolite™ F300

Among the first commercially available MOFs are Basolite™ A100 and Basolite™ F300, produced by BASF SE and sold by Sigma Aldrich. Both are classified as hydrophilic with a reactivation temperature of 200 °C.

Basolite™ A100 is identical to MIL-53(Al).[73] Similar to that of MIL-53(Cr),[74] the water adsorption capacity of MIL-53(Al) is not comparable to that of MIL-100 or MIL-101. Whereas MIL-53(Cr) shows a large plateau with a loading of approximately 0.1 g g^{-1} over nearly the whole relative pressure range, as reported by Bourrelly et al.,[74] the commercially available MIL-53(Al) has a higher adsorption capacity (see Figure 12).

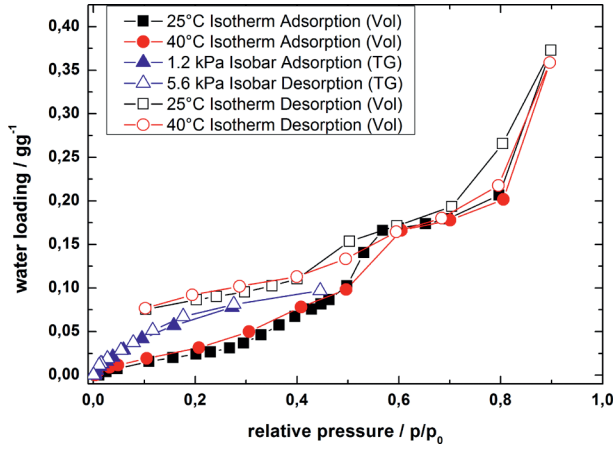

Figure 12. Water adsorption characteristics of Basolite™ A100.

Adsorption occurs comparatively late in MIL-53; this has been explained by the fact that two forms of the material exist: narrow- and open pore. The narrow-pore form is favored during the introduction of water molecules.[57] Therefore, the pores of the flexible framework remain closed up to a certain concentration, as this is favored by water–framework interaction energies.

Basolite™ F300 is an iron(III) trimesate with a bulk density of 0.35 cm^3 g^{-1} and a BET surface area of 1300–1600 m^2 g^{-1}. Its porosity and composition are in agreement

with those of MIL-100(Fe), but the structure of Basolite™ F300 is different and is still unknown or undisclosed.[75] Relative to those of Basolite™ A100, the water adsorption measurements performed with this material showed quite interesting results. The isotherms show a more hydrophilic behavior, with an uptake of up to 0.4 g g^{-1} in a low relative pressure range (see Figure 13).

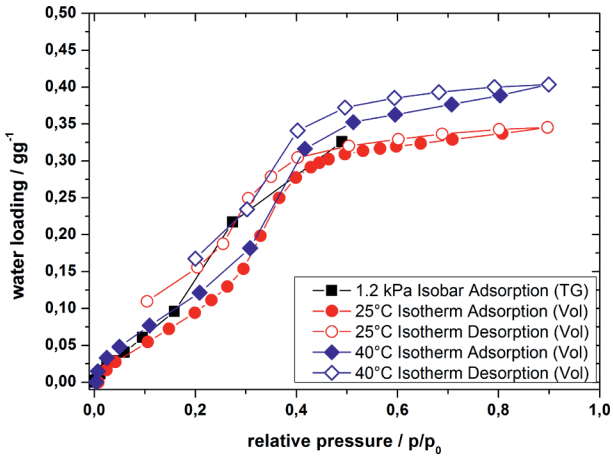

Figure 13. Water adsorption characteristics of Basolite™ F300.

Evaluation of ZMOFs/ZIFs

With regard to the required high hydrothermal stability, zeolite-like MOFs (ZMOFs) and zeolitic imidazolate frameworks (ZIFs) may serve as a bridge between the higher uptake but lower stability of pure MOFs and the higher hydrothermal stability but lower uptake of zeolites. In case of ZMOFs, simulated water adsorption isotherms of different ion-exchanged ZMOFs were very promising, with loadings of up to 0.34 g g^{-1}.[76] The commercially available Basolite™ Z1200, a candidate out of this class with a ZIF-8 structure, was evaluated.[77,78] In accordance with the literature, the water adsorption isotherms show hydrophobic character with almost no water uptake. This behavior is similar to that of other ZIF materials, for example, the ZIF-71 with a hydrophobic cage and a strong hysteresis loop.[79] However, as shown very recently for the zinc 2-methylimidazolate MAF-4, such structures can be tuned to become hydrophilic.[80] By replacing the 2-methylimidazolate linker partially or entirely with 3-methyl-1,2,4-triazolate, Zhang and co-workers were able to influence the polarity of the material strongly, as the additional nitrogen atom in the triazolate served as an extra active site for the adsorption of polar molecules. This increased the water loading from 0.056 g g^{-1} to 0.38 g g^{-1} and moved the capillary condensation step to relative pressures as little as p/p_0 = 0.2–0.3 in the entirely substituted MAF-7 material. Although the material adsorbs irreversibly a water loading of 0.056 g g^{-1}, this experiment impressively demonstrates the potential of material tailoring.

Heat of Adsorption and Cycle Stability

In addition to the water uptake, another important figure is the heat of adsorption (HoA). In the cooling application, the heat of adsorption must be released to the environment and should therefore be as low as possible. On the contrary, in the heat storage or heat pump application, this is also useful heat and directly connected to heating performance. In addition, the hydrothermal cycle stability is an essential and, for several MOFs, the most critical requirement with regard to applications. A brief overview on the maximum water adsorption capacities at given relative pressures and heats of adsorption for the samples discussed in this work is given in Table 1.

Table 1. Summary of the discussed materials and their relevant data.

Compound	Water uptake /g g^{-1}	p/p_0	HoA /kJ mol^{-1}	Source
MIL-101(Cr)	1.01	0.921	46.0–47.2[a]	[60]
MIL-101(Cr)	1.43	0.916	–	This work
MIL-101(Cr)	1.37	0.978	45.13[b]	[48]
MIL-100(Fe)	0.651	0.9	48.83[b]	[48]
MIL-100(Cr) (X = Cl)	0.671	0.48	47.6–47.9[b]	[71]
MIL-100(Cr) (X = F)	0.614	0.47	47.7–49.0[b]	[71]
MIL-100(Cr) (X = 0.5SO$_4$)	0.611	0.49	47.9–49.1[b]	[71]
HKUST-1	0.418	0.367	50.7[a]	This work and ref.[11]
HKUST-1	0.55	0.9	–	[48]
ISE-1	0.21	0.4	43.92[a]	[66]
Basolite™ C300	0.6	0.7	46.6[a]	This work
Basolite™ A100	0.2	0.8	52.1[a]	This work
Basolite™ F300	0.3	0.4	47.6[a]	This work

[a] Direct measurements TG/DSC. [b] Calculated from two isotherms.

The achievable water uptake is in the range 0.2 g g^{-1} for the commercial Basolite™ A100 up to over 1.4 g g^{-1} for a MIL-101. The heat of adsorption was determined either by direct measurement within a simultaneous thermogravimetry/differential scanning calorimeter (TG/DSC) on the basis of the Tian–Calvet principle or by calculation from two volumetric isotherms performed at different temperatures.

For the commercially available MOFs, first cycling stability tests were performed with a thermogravimetric apparatus at a constant water partial pressure of 5.6 kPa. The samples were treated for 20 cycles by varying the temperature from 40 to 140 °C. The water loading was measured before and after the cycles. The results of the cycling stability test are shown in Table 2.

Unfortunately, all evaluated commercial samples show some degradation during and after the hydrothermal cycle, which manifests itself in a loss of water loading capacity. In case of the HKUST-1 sample, the capacity is reduced by 53%, relative to the initial uptake. In addition, a slight increase in the dry mass can be observed. Basolite™ A100 and Basolite™ Z1200 show no dramatic loss, however the desorption process is extremely slow in both cases. How-

Table 2. Summary of the performed cycle stability tests on Basolite™.

Compound	Loading /g g^{-1}	Dry mass /mg	Loading[a] /g g^{-1}	Dry mass[a] /mg
Basolite™ C300	0.55	81.0	0.26	83.4[b]
Basolite™ A100	0.008	86.2	0.007	85.4[c]
Basolite™ F300	0.34	85.4	0.10	85.7
Basolite™ Z1200	0.008	96.9	0.007	96.2[c]

[a] After 20 cycles. [b] Structural change under water atmosphere. [c] Slow drying process: loss of water over the whole measurement under measurement conditions.

ever, the water uptake under the cycle conditions is very poor. Basolite™ F300 shows a dramatic loss of capacity, with a reduction of more than 74% of the initial loading.

Conclusion

As a result of this work and in agreement with the literature, the new family of MOFs can be considered as a very promising class of materials for use in adsorption heat transformation processes. Several compounds with large water uptakes up to 1.43 g g^{-1} have been identified. This is more than four times the maximum loading of conventionally used zeolites. With regard to the application, the adsorption step of several MOFs occurs at a high relative pressure ($p/p_0 > 0.35$), which reduces the useful loading lift within the possible cycle. In addition, the most critical issue is the hydrothermal stability of the network. Several compounds show a large degradation within a few cycles.

However, these materials are very promising, as there are first promising stability results for MIL-101 and MIL-100. In addition, the modular concept allows their physical properties to be tuned in accordance with the desired application boundary conditions in a wide range. A clear advantage of MOFs over conventional zeolite-type sorbents is the variability of the hydrophilicity of the network through the organic linker or the metal cluster, which creates room for further improvements and may render MOFs the sorbents of choice in the future.

Acknowledgments

Funding by the Federal German Ministry of Economics (BMWi) under grant 0327851A/B is gratefully acknowledged.

[1] R. E. Critoph, Y. Zhong, *Proc. IMechE: Part E: J. Process Mechanical Eng.* **2005**, *219*, 285–300.
[2] H. Henning, *Appl. Therm. Eng.* **2007**, *27*, 1734–1749.
[3] M. Pons, F. Meunier, G. Cacciola, R. Critoph, M. Groll, L. Puigjaner, B. Spinner, F. Ziegler, *Int. J. Refrig.* **1999**, *22*, 5–17.
[4] F. Ziegler, *Int. J. Therm. Sci.* **1999**, *38*, 191–208.
[5] F. Ziegler, *Int. J. Refrig.* **2002**, *25*, 450–459.
[6] T. Núñez, W. Mittelbach, H.-M. Henning, *Appl. Therm. Eng.* **2007**, *27*, 2205–2212.
[7] H. Demir, M. Mobedi, S. Ülkü, *Renewable Sustainable Energy Rev.* **2008**, *12*, 2381–2403.
[8] J. Deng, R. Z. Wang, G. Y. Han, *Prog. Energy Combust. Sci.* **2011**, *37*, 172–203.
[9] Y. I. Aristov, G. Restuccia, G. Cacciola, V. Parmon, *Appl. Therm. Eng.* **2002**, *22*, 191–204.
[10] E.-P. Ng, S. Mintova, *Microporous Mesoporous Mater.* **2008**, *114*, 1–26.
[11] S. K. Henninger, F. P. Schmidt, H.-M. Henning, *Appl. Therm. Eng.* **2010**, *30*, 1692–1702.
[12] C. Janiak, *Angew. Chem.* **1997**, *109*, 1499; *Angew. Chem. Int. Ed. Engl.* **1997**, *36*, 1431–1434.
[13] H. Li, M. Eddaoudi, M. O'Keeffe, O. M. Yaghi, *Nature* **1999**, *402*, 276–279.
[14] O. M. Yaghi, M. O'Keeffe, N. W. Ockwig, H. K. Chae, M. Eddaoudi, J. Kim, *Nature* **2003**, *423*, 705–14.
[15] J. Rowsell, O. M. Yaghi, *Microporous Mesoporous Mater.* **2004**, *73*, 3–14.
[16] G. Férey, C. Mellot-Draznieks, C. Serre, F. Millange, J. Dutour, S. Surblé, I. Margiolaki, *Science* **2005**, *309*, 2040–2042.
[17] G. Férey, *Chem. Soc. Rev.* **2008**, *37*, 191–214.
[18] G. Férey, C. Serre, *Chem. Soc. Rev.* **2009**, *38*, 1380–1399.
[19] G. Férey, *Dalton Trans.* **2009**, 4400–4415.
[20] R. J. Kuppler, D. J. Timmons, Q.-R. Fang, J.-R. Li, T. A. Makal, M. D. Young, D. Yuan, D. Zhao, W. Zhuang, H.-C. Zhou, *Coord. Chem. Rev.* **2009**, *253*, 3042–3066.
[21] K. Hindson, *Eur. J. Inorg. Chem.* **2010**, 3683.
[22] S. Kitagawa, S. Natarajan, *Eur. J. Inorg. Chem.* **2010**, 3685.
[23] A. U. Czaja, N. Trukhan, U. Müller, *Chem. Soc. Rev.* **2009**, *38*, 1284–93.
[24] U. Mueller, M. Schubert, F. Teich, H. Puetter, K. Schierle-Arndt, J. Pastré, *J. Mater. Chem.* **2006**, *16*, 626–636.
[25] Z. Chen, S. Xiang, H. D. Arman, P. Li, S. Tidrow, D. Zhao, B. Chen, *Eur. J. Inorg. Chem.* **2010**, 3745–3749.
[26] F. Ma, S. Liu, D. Liang, G. Ren, C. Zhang, F. Wei, Z. Su, *Eur. J. Inorg. Chem.* **2010**, 3756–3761.
[27] J.-R. Li, Y. Ma, M. C. McCarthy, J. Sculley, J. Yu, H.-K. Jeong, P. B. Balbuena, H.-C. Zhou, *Coord. Chem. Rev.* **2011**, *255*, 1791–1823.
[28] D. Liu, C. Zhong, *J. Mater. Chem.* **2010**, *20*, 10308–10318.
[29] L. J. Murray, M. Dincă, J. R. Long, *Chem. Soc. Rev.* **2009**, *38*, 1294–314.
[30] J.-R. Li, R. J. Kuppler, H.-C. Zhou, *Chem. Soc. Rev.* **2009**, *38*, 1477–504.
[31] G. Férey, C. Serre, T. Devic, G. Maurin, H. Jobic, P. L. Llewellyn, G. De Weireld, A. Vimont, M. Daturi, J.-S. Chang, *Chem. Soc. Rev.* **2011**, *40*, 550–62.
[32] S. K. Nune, P. K. Thallapally, B. P. McGrail, *J. Mater. Chem.* **2010**, *20*, 7623–7625.
[33] D. Farrusseng, S. Aguado, C. Pinel, *Angew. Chem.* **2009**, *121*, 7638; *Angew. Chem. Int. Ed.* **2009**, *48*, 7502–7513.
[34] J. Lee, O. K. Farha, J. Roberts, K. A. Scheidt, S. T. Nguyen, J. T. Hupp, *Chem. Soc. Rev.* **2009**, *38*, 1450–1459.
[35] L. Ma, C. Abney, W. Lin, *Chem. Soc. Rev.* **2009**, *38*, 1248–56.
[36] T. Ladrak, S. Smulders, O. Roubeau, S. J. Teat, P. Gamez, J. Reedijk, *Eur. J. Inorg. Chem.* **2010**, 3804–3812.
[37] W. Kleist, F. Jutz, M. Maciejewski, A. Baiker, *Eur. J. Inorg. Chem.* **2009**, 3552–3561.
[38] M. D. Allendorf, C. A. Bauer, R. K. Bhakta, R. J. T. Houk, *Chem. Soc. Rev.* **2009**, *38*, 1330–52.
[39] C. Janiak, T. G. Scharmann, P. Albrecht, F. Marlow, R. Macdonald, *J. Am. Chem. Soc.* **1996**, *118*, 6307–6308.
[40] H. A. Habib, A. Hoffmann, H. A. Hoeppe, G. Steinfeld, C. Janiak, *Inorg. Chem.* **2009**, *48*, 2166–2180.
[41] M. Kurmoo, *Chem. Soc. Rev.* **2009**, *38*, 1353–79.
[42] B. Gil-Hernandez, P. Gili, J. K. Vieth, C. Janiak, J. Sanchiz, *Inorg. Chem.* **2010**, *49*, 7478–7490.
[43] H. A. Habib, J. Sanchiz, C. Janiak, *Inorg. Chim. Acta* **2009**, *362*, 2452–2460.
[44] C. Janiak, *Dalton Trans.* **2003**, 2781.
[45] V. Kaučič, *Nachr. Chem.* **2011**, *59*, XII–XVI.
[46] M. Rosseinsky, *Microporous Mesoporous Mater.* **2004**, *73*, 15–30.

[47] J. J. Low, A. I. Benin, P. Jakubczak, J. F. Abrahamian, S. A. Faheem, R. R. Willis, *J. Am. Chem. Soc.* **2009**, *131*, 15834–42.
[48] P. Küsgens, M. Rose, I. Senkovska, H. Fröde, A. Henschel, S. Siegle, S. Kaskel, *Microporous Mesoporous Mater.* **2009**, *120*, 325–330.
[49] S. Kitagawa, R. Kitaura, S.-I. Noro, *Angew. Chem.* **2004**, *116*, 2388; *Angew. Chem. Int. Ed.* **2004**, *43*, 2334–75.
[50] C. Janiak, J. K. Vieth, *New J. Chem.* **2010**, *34*, 2366–2388.
[51] D. J. Tranchemontagne, J. L. Mendoza-Cortés, M. O'Keeffe, O. M. Yaghi, *Chem. Soc. Rev.* **2009**, *38*, 1257–83.
[52] M. O'Keeffe, *Chem. Soc. Rev.* **2009**, *38*, 1215–1217.
[53] S. Kaskel, *Chem. Ing. Tech.* **2010**, *82*, 1019–1023.
[54] M. Thommes, *Chem. Ing. Tech.* **2010**, *82*, 1059–1073.
[55] D. Tanaka, K. Nakagawa, M. Higuchi, S. Horike, Y. Kubota, T. C. Kobayashi, M. Takata, S. Kitagawa, *Angew. Chem.* **2008**, *120*, 3978; *Angew. Chem. Int. Ed.* **2008**, *47*, 3914–3918.
[56] F. Coudert, M. Jeffroy, A. Fuchs, *J. Am. Chem. Soc.* **2008**, *130*, 14294–14302.
[57] D. S. Coombes, F. Cora, C. Mellot-Draznieks, R. G. Bell, *J. Phys. Chem. C* **2009**, *113*, 544–552.
[58] S. K. Henninger, G. Munz, K.-F. Ratzsch, P. Schossig, *Renewable Energy* **2011**, *36*, 3043–3049.
[59] J. A. Greathouse, M. D. Allendorf, *J. Am. Chem. Soc.* **2006**, *128*, 10678–10679.
[60] J. Ehrenmann, S. K. Henninger, C. Janiak, *Eur. J. Inorg. Chem.* **2011**, 471–474.
[61] S. K. Henninger, PhD Thesis, Albert-Ludwigs-Universität Freiburg, **2007**.
[62] S. S.-Y. Chui, S. M.-F. Lo, J. P. H. Charmant, A. G. Orpen, I. D. Williams, *Science* **1999**, *283*, 1148–1150.
[63] A. Vishnyakov, P. I. Ravikovitch, A. V. Neimark, M. Bülow, Q. M. Wang, *Nano Lett.* **2003**, *3*, 713–718.
[64] J. M. Castillo, T. J. H. Vlugt, S. Calero, *J. Phys. Chem. C* **2008**, *112*, 15934–15939.
[65] L. Grajciar, O. Bludsky, P. Nachtigall, *J. Phys. Chem. Lett.* **2010**, *1*, 3354–3359.
[66] S. Henninger, F. Schmidt, H.-M. Henning, *Adsorption* **2011**, *17*, 833–843.
[67] S. K. Henninger, G. Munz, S. Müller, K.-F. Ratzsch, P. Schossig, H.-M. Henning in *Proc. 1st Int. Conf. Materials for Energy*, Karlsruhe, Germany, **2010**.
[68] K. Schlichte, T. Kratzke, S. Kaskel, *Microporous Mesoporous Mater.* **2004**, *73*, 81–88.
[69] S. K. Henninger, H. A. Habib, C. Janiak, *J. Am. Chem. Soc.* **2009**, *131*, 2776–2777.
[70] G. Férey, C. Serre, C. Mellot-Draznieks, F. Millange, S. Surblé, J. Dutour, I. Margiolaki, *Angew. Chem.* **2004**, *116*, 6456; *Angew. Chem. Int. Ed.* **2004**, *43*, 6296–301.
[71] G. Akiyama, R. Matsuda, S. Kitagawa, *Chem. Lett.* **2010**, *39*, 360–361.
[72] P. Horcajada, S. Surblé, C. Serre, D.-Y. Hong, Y.-K. Seo, J.-S. Chang, J.-M. Grenèche, I. Margiolaki, G. Férey, *Chem. Commun.* **2007**, 2820–2822.
[73] F. Millange, C. Serre, G. Férey, *Chem. Commun.* **2002**, 822–823.
[74] S. Bourrelly, B. Moulin, A. Rivera, G. Maurin, S. Devautour-Vinot, C. Serre, T. Devic, P. Horcajada, A. Vimont, G. Clet, M. Daturi, J.-C. Lavalley, S. Loera-Serna, R. Denoye, P. L. Llewellyn, G. Férey, *J. Am. Chem. Soc.* **2010**, *132*, 9488–98.
[75] A. Centrone, E. E. Santiso, T. A. Hatton, *Small* **2011**, *7*, 2356–2364.
[76] A. Nalaparaju, R. Babarao, X. Zhao, J. Jiang, *ACS Nano* **2009**, *3*, 2563–2572.
[77] K. S. Park, Z. Ni, A. P. Côté, J. Y. Choi, R. Huang, F. J. Uribe-Romo, H. K. Chae, M. O'Keeffe, O. M. Yaghi, *PNAS.* **2006**, *103*, 10186–91.
[78] X.-C. Huang, Y.-Y. Lin, J.-P. Zhang, X.-M. Chen, *Angew. Chem.* **2006**, *118*, 1587; *Angew. Chem. Int. Ed.* **2006**, *45*, 1557–1559.
[79] A. Nalaparaju, X. Zhao, J. Jiang, *J. Phys. Chem. C* **2010**, *114*, 11542–11550.
[80] J.-P. Zhang, A.-X. Zhu, R.-B. Lin, X.-L. Qi, X.-M. Chen, *Adv. Mater.* **2011**, *23*, 1268–71.

Received: October 4, 2011
Published Online: December 13, 2011

